Nb Superconducting Hot Electron Bolometer Mixers Coupled with Microstrip Lines

Walter F. M. Ganzevles, Pavel Yagoubov, Jian Rong Gao, Teun M. Klapwijk and Piet A. J. de Korte

Abstract— **The measured direct and heterodyne response of a quasi-optically coupled superconducting Nb hot-electron bolometer mixer (HEBM) at 2.5 THz is reported. This mixer exploits a novel coupling circuit in which the microstrip line transformer is used to feed the rf signal from the twin slot antenne to the microbridge. The microstrip line is made of $Au/SiO_2/Al$. Using a Fourier transform spectrometer, the frequency response of such a device is measured. We find a peak response at a frequency of 1.9 THz, which is 20% lower than predicted, and a bandwidth of 1.6 THz as we expect. By applying 2.5 THz radiation from a far infrared laser, we measure an uncorrected noise temperature $T_{N,rec}$ of 4200 K.**

Keywords— **Superconducting device, hot-electron bolometer mixer, microstrip line, submillimeter radio astronomy.**

I. Introduction

SUPERCONDUCTING HEBMs are very promising candidates to fulfill the need for low-noise, high frequency detectors in satellite-based astronomical missions. Practical application of these devices requires a suitable antenna like a twin slot antenna. To match the antenna-impedance to the bridge impedance, a transmission line is needed. In the literature, the use of Co-Planar Waveguide (CPW) transmission lines at 2.5 THz is reported [1], [2]. An alternative is to use microstrip transmission lines. So far, this coupling structure has only been used for superconductor -isolator-superconductor (SIS) mixers but never for HEBMs.

There are various reasons to try microstrip lines instead of CPW-transmission lines in THz HEBMs. First, it allows for a much larger variation in characteristic impedance of the transmission line, making it easier to match a diffusion cooled HEB, which usually has a low impedance. Second, the microstrip transmission line has proven to work very well in an SIS-mixer up to about 1 THz [3], [4]. Simulation models are well developed, where CPW calculations have proven to be difficult, particularly for structures having very small slots. Third, the presence of a microstrip line is expected not to disturb the antenna beam pattern. In a CPW-design however, there is such a disturbance due to the fact that all other structures are also situated in the ground plane. Last, with respect to the fabrication, the microstrip lines could be easier than CPW transmission line because the former structures can be defined by conventional optical lithography. There is no need for high-resolution lithography such as e-beam lithography as required for CPW transmission lines.

In this paper, we start with the description of our mixers followed by their fabrication. Then we report measurements on the direct response, which we compare to a model predicting its frequency response. We also report our preliminary noise measurement at 2.5 THz. We end with a discussion and conclusion.

Manuscript received September 15, 2000. This work is financially supported by the Stichting voor Technische Wetenschappen, which is part of the Nederlandse Organisatie voor Wetenschappelijk Onderzoek and, by ESA under contract no. 11738/95/NL/PB. W. F. M. Ganzevles and T. M. Klapwijk are with the Department of Applied Physics and Delft Institute for Microelectronics and Submicron Technology (DIMES), Delft University of Technology, Lorentzweg 1, 2628 CJ Delft, The Netherlands. P. Yagoubov, J. R. Gao, and P. A. J. de Korte are with the Space Research Organization of the Netherlands, Sorbonnelaan 2, 3584 CA Utrecht, The Netherlands. Corresponding authors' E-mail: walter@sron.rug.nl.

II. Experiments

A. Device Lay-out

Fig. 1 shows a scanning electron micrograph of the device used. The twin slot antenna is formed by the two dark vertical lines in the ground plane. The three rectangles are the SiO_2 dielectric. On this dielectric layer, the top wiring is defined. Together with the SiO_2 and the ground plane, this forms the microstrip line. The radial stubs act as an rf short to the ground. The Nb microbridge is located between the two tapered cooling pads. The IF contact is made by a CPW transmission line which is not shown in this figure.

B. Sample Fabrication

A fabrication process for Nb HEBMs has been developed using two-step electron beam lithography (EBL) to

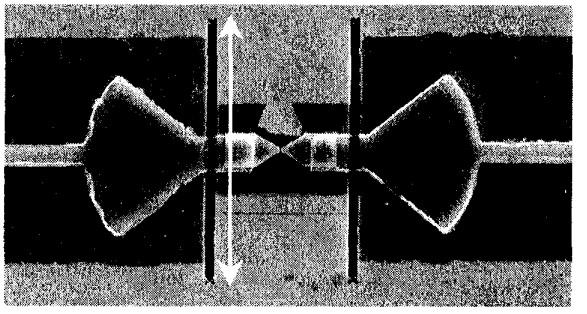

Fig. 1. Scanning electron micrograph of a microstrip line-coupled HEBM. The arrow indicates 31 μm. The 2 dark vertical lines in the ground plane are the antenna slots. On top of the big SiO_2 rectangles, the Al/Nb top wiring is visible. Radial stubs serve as rf shorts to the ground plane, picking up radiation from the antenna. They also form the first section of the rf filter. The triangles form the cooling pads, defining the bridge length.

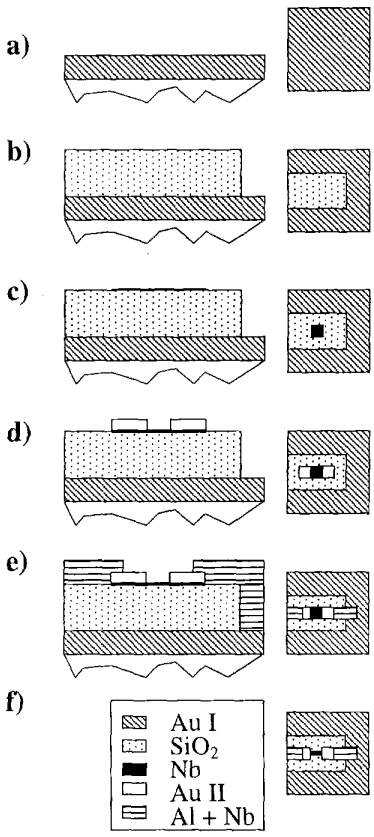

Fig. 2. A process flow in schematic cross-sectional (left) and top view (right).

define both bridge length and width. Near UV lithography is used to define the rest of the device. We use a high-resistivity, double-sided polished Si substrate. In the first step, a ground plane of 250 nm thick Au is evaporated (Fig. $2^{a)}$). The ground plane contains the twin slot antenna and the intermediate frequency (IF) CPW as well as alignment markers for consecutive steps. In a lift-off process, a dielectric of 250 nm SiO_2 is sputtered on the areas where the microstrip line will be located ($2^{b)}$). Then we deposit 16 nm thick Nb using dc sputtering, as indicated in $2^{c)}$. Using a lift-off mask, patches of 12 μm $\times$ 12 μm on top of the SiO_2 are covered. Au cooling pads are then defined by EBL using a double layer PMMA system ($2^{d)}$). The cooling pads are formed in two steps: $\sim$ 10 nm Au is dc sputtered. In a different machine, 80 nm Au is e-beam evaporated. Before the sputtering of the Au, the native oxide of the Nb is removed with rf Ar etching in order to achieve a high transparency between the Nb and the Au. The top wiring ($2^{e)}$) of the microstrip line is a layer of 550 nm Al, on top of which 75 nm Nb is sputtered to reduce dc- and IF series resistance. This top wiring is defined in an optical lift-off process. Again to avoid loss at IF, 90 nm Nb is deposited on the IF CPW-transmission line using a optically defined lift-off mask. In the last production step ($2^{f)}$, no cross section shown), we define the bridge width. Using EBL, we define a PMMA bridge in the double layer resist system as before. Only the Nb parts that have to be etched are opened up. In a mixture of CF_4+3% O_2, the Nb is reactive ion etched. We monitor the process by measuring the optical reflectivity of the Nb on the SiO_2 using a laser interferometer as an endpoint detection system. In this process we are able to produce Nb bridges as small as 60 nm$\times$ 80 nm [5].

In this process, achieving contact between the top wiring and the ground plane is the bottleneck. In contrast to the typical SIS devices [4], the superconducting bridge acts as part of the top wiring. This means an electrical contact between the top wiring and the ground plane is needed. This is established via a step coverage on the vertical wall of the SiO_2 (Fig. $2^{e)}$), which turns out to be rather difficult. We overcome this problem by sputter depositing a *thick* (625 nm Al/Nb) wiring layer.

A typical device has a critical current density of 2×10^{10} Am^{-2} and a critical temperature T_c of 5 K. The 16 nm thick Nb film has a square resistance of 25 Ω.

C. Direct Response

The direct response in current $\Delta I(f)$ of an HEBM measured in a Fourier Transform Spectrometer (FTS) can be described by

$$\Delta I(f) \propto \eta_{\text{int}} \cdot \eta_{\text{opt}} \cdot \eta_{\text{FTS}}, \tag{1}$$

with η_{opt} the combined transmission of the window and heat filter and η_{FTS} the power transfer function of the FTS [2], [8].

Fig. 3 shows a measured response $\Delta I(f)$ of the device measured with an FTS at a bath temperature of $T_{\text{bath}} = 3$ K. Details of the measurement setup have been described elsewhere [8]. The dip observed at 2.1 THz is due to absorption in a polyethylene lens in the setup. This lens is used to optimize the signal level. We simulated the Gaussian coupling efficiency of the beam from FTS to that of the device. The frequency dependence of this system in the range 0.5 THz to 4 THz is only weak. The measured 3 dB-bandwidth B_m equals 1.6 THz and $f_{center,m}$ is found to be 1.9 THz. We also calculate the response using a real device geometry. The plot also shows the predicted response $\eta_{\text{int,sim}} \cdot \eta_{\text{opt}} \cdot \eta_{\text{FTS}}$ with $B_{\text{sim}} = 1.2$ THz and $f_{\text{center,sim}} = 2.3$ THz. Similar data have been obtained from several devices. The data are well described by the model except for a 20% downshift of the peak response. This downshift has also been observed in CPW-based devices.

To understand the measurement, we simulate the direct response of the HEBM. To do so, we first have to know the frequency dependence of the windows and transmission of the FTS, $\eta_{\text{opt}} \cdot \eta_{\text{FTS}}$. The product $\eta_{\text{opt}} \cdot \eta_{\text{FTS}}$, determined previously, [8] is also included in Fig. 3. To calculate the η_{int}, we choose an approach based on the coupling of impedances [7]. Generally, the impedance of a transmission line of length l, propagation constant γ and characteristic

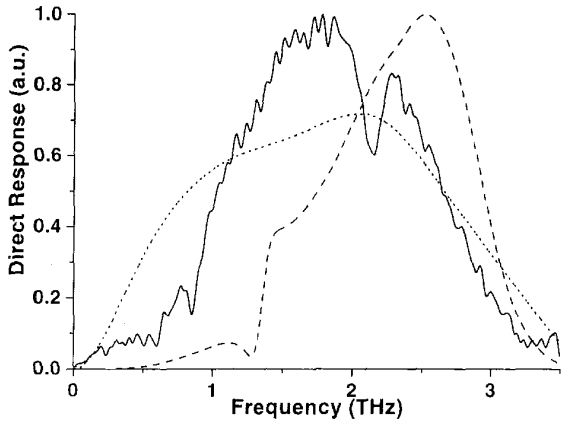

Fig. 3. Direct response as a function of frequency of a typical microstrip line coupled HEB together with the transmission of the Fourier transform spectrometer and optics. Shown are the normalized measured data (solid), transmission of the optics and FTS $\eta_{\rm opt} \cdot \eta_{\rm FTS}$ (dotted) and relative simulated response $\eta_{\rm int,sim} \cdot \eta_{\rm opt} \cdot \eta_{\rm FTS}$ (dashed). $\eta_{\rm int,sim}$ takes into account different conductivities for top- and bottom layer, geometry of the cooling pads and transmission of the FTS.

impedance $Z_{\rm line}$ terminated by a load $Z_{\rm load}$ is given by

$$Z_{\rm embed} = Z_{\rm line} \frac{Z_{\rm load} + iZ_{\rm line} \tan(\gamma \cdot l)}{Z_{\rm line} + iZ_{\rm load} \tan(\gamma \cdot l)}. \quad (2)$$

We calculate the impedance of the antenna, microstrip line filter and transformer separately. We then use (2) to determine the impedance at the position of the Nb bridge. The power transfer from the antenna to the bridge is then calculated using

$$\eta_{\rm int} = 1 - \left| \frac{Z_{\rm HEB} - Z_{\rm embed}}{Z_{\rm HEB} + Z_{\rm embed}} \right|^2. \quad (3)$$

To obtain the impedance of the elements, we first consider the microbridge itself. We assume its impedance Z_{HEB} can be expressed as $Z_{\rm HEB} = R_N$ [2] with R_N the normal state resistance. Second, the impedance of the antenna as a function of frequency is calculated using a moment method in the Fourier transform domain, developed by Kominami, Pozar and Schaubert [6]. For details, see [2] and [8]. Third, the impedance of the microstrip line elements is calculated based on a model used for microstrip line calculations (see e.g. [9] and [10]). We calculate the surface resistance of both Au and Al in the extreme anomalous limit. The characteristic impedance of the line is calculated as a function of frequency, line width and thickness of top- and bottom metal layers and the dielectric. By varying these parameters, the impedance can be tuned from about 5 Ω to 35 Ω without introducing orthogonal modes, i.e. without making the line wider than about $\lambda/4$. The key part of the microstrip line is the transformer. It matches the effective antenna- and filter impedance $Z_{\rm embed}$ to the impedance of the bridge following equation (2).

The transmission of the rf choke filter, avoiding rf signal to be lost into the dc- or IF chain, is calculated using the characteristic impedance of each section (found using the same calculations as the transformer) and repeated application of (2).

In the simulations shown in Fig. 3, we use a top layer dc conductivity $\sigma_{top} = 5 \cdot 10^7\ \Omega^{-1}m^{-1}$ and $\sigma_{bottom} = 2 \cdot 10^8\ \Omega^{-1}m^{-1}$ for the ground plane. These values are measured on films similar to the ones in the device.

We have also measured several devices with a slightly different design regarding the top wiring layer. Devices having a rectangular coupler instead of a radial stub (Fig. 1) do not show significant deviations in the observed direct response. On the other hand, a device having a filter with 6 $\lambda/4$ sections (instead of 2 sections as in the device discussed in this work) on either side shows a larger bandwidth (1.9 THz) and a lower $f_{\rm center}$ (1.5 THz).

D. Heterodyne Response

Heterodyne measurements are performed at 2.5 THz using a FIR laser as a local oscillator (LO). Applying this laser in combination with a 6 μm Mylar beam splitter it is possible to pump the IV curves of the devices flat. Although the stability of the output power from laser is on the order of 0.1%/min, measured using a pyro-detector, we find it still difficult to measure the Y-factor in a unchopped mode due to instabilities in coupling of the LO power to the HEBM. To average out these instabilities, we use a chopped hot/cold load at 300K/77K. At the IF, both the ac amplitude and dc component of the power, P_{ac} and P_{dc}, respectively, are recorded. From the Y-factor, $Y = \frac{(P_{dc}+\alpha \cdot P_{ac})}{(P_{dc}-\alpha \cdot P_{ac})}$, the receiver noise temperature can be determined [11]. α is a numerical factor ranging from 1 to 1.4, depending on the setup used. Since its value is not known for our experiment, we used $\alpha = 1$ to determine the noise temperature, giving a worst case-value for the noise temperature.

The IF-chain consists of a standard bias T, isolator and HEMT amplifier and has 79 dB gain and a noise temperature of less than 7 K in the band from 1.2 to 1.7 GHz.

Fig. 4 shows the unpumped, optimally pumped and overpumped IV curves of the mixer, taken at a bath temperature of 2.8 K. The thin dashed line represents the Y-factor as a function of bias voltage. An optimal, chopped Y-factor of 0.22 $\pm$ 0.05 dB has been measured. This corresponds to an uncorrected noise temperature $T_{\rm N,\ uncorr}$ of 4200 $\pm$ 1000 K. It is checked that this peak is not due to oscillations in the bias circuitry nor to direct detection. This noise temperature is a few times the best noise temperature measured so far with a diffusion-cooled HEBM using CPW transmission line [11]. A receiver gain of -23 dB has been measured using the ratio of differences in rf input power between the hot and cold black body and the corresponding difference at the IF port *of the mixer.*

III. Discussion

Although it was anticipated that the fabrication of microstrip line coupled HEBMs would be easier than that of the CPW-coupled version, contacting the top wiring to the

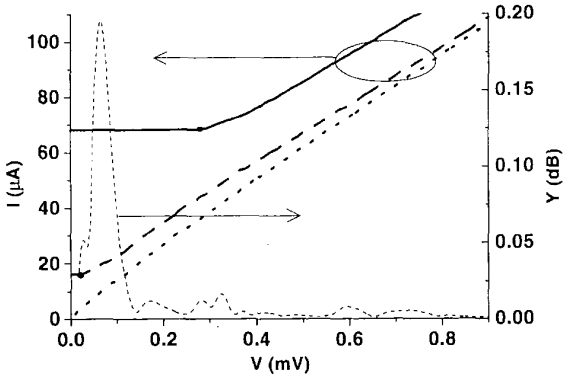

Fig. 4. IV-curves of the HEBM pumped with 2.5THz-radiation: unpumped (solid) IV curve, optimally pumped (dashed) and overpumped (dotted) measured at 2.8 K, IF=1.25 GHz. The thin dashed line shows the chopped Y-factor in the optimally pumped situation.

ground plane (see (Fig. 2^e)) is a challenge. This is because the SiO_2 tends to form high and sharp edges after lift off. These make it very hard to obtain a good step coverage across the dielectric to the ground plane. A thick, sputter-deposited top wiring turns out to be a solution.

Initially, the coupling structure used in this work was designed for a center frequency of 2.5 THz. Our experimental data show that the measured center frequency is 20% lower than predicted based by the model taking the actual device parameters into account. Devices based on a similar antenna but having a CPW transformer have shown a similar downshift in frequency [2]. A similar effect has been reported in CPW-based structures [1]. It was suggested [2] that, in the CPW design, the thickness of the metal layers in the structure should be taken into account. Another proposal by Wyss et al. [12] is the sudden decrease in line width from the transformer to the –much narrower– microbridge. We explored this hypothesis by simulating microstrip line devices with such a decrease in line width. Indeed, for realistic geometries, a downshift of 10 to 15% is observed.

Assuming the source of the downshift is recognized, the model for describing the direct response works well. This may suggest that the model used for the calculation of the impedance of microstrip line works up to a few THz. As far as we know, this is the first demonstration of using microstrip lines at a few THz.

A question that can be raised is which coupling scheme leads to the best sensitivity of a THz HEBM. We are not able to draw a conclusion based on these preliminary measurements. The answer has to come from a detailed experimental comparison between CPW- and microstrip line devices.

IV. Conclusions

In this work we have shown the fabrication of a novel coupling scheme for quasi-optically coupled HEBMs. Measurements of the direct response are compared to model calculations, and agree reasonably well, except for an offset of 15 to 20%. Possible mechanisms for this offset are discussed. Heterodyne measurements show a noise temperature of 4200 ± 1000 K.

Acknowledgment

The authors thank Maarten Stokhof and Anja van Langen for their help in sample production, Willem-Jan Vreeling for technical support in setting up the laser and Pierre Echternach for interesting discussion.

References

[1] B. S. Karasik, M. C. Gaidis, W. R. McGrath, B. Bumble and H. G. LeDuc, "A low-noise 2.5 THz superconductive Nb hot-electron mixer," *IEEE Trans. on Appl. Supercond.*, vol. 7, pp. 3580-3583, June 1997.

[2] W. F. M. Ganzevles, L. R. Swart, J. R. Gao, T. M. Klapwijk and P. A. J. de Korte, "Direct response of twin slot antenna coupled hot-electron bolometer mixers designed for 2.5 THz radiation detection," *Appl. Phys. Lett.* vol. 76, pp. 3304-3306, July 2000, and references therein.

[3] J. Zmuidzinas and H. G. LeDuc, "Quasi-optical slot antenna SIS mixers," *IEEE Trans. on Microwave Theory Techn.* vol. 40, pp. 1797-1804, September 1992.

[4] M. Bin, M. C. Gaidis, J. Zmuidzinas, T. G. Phillips and H. G. LeDuc, "Low-noise 1 THz niobium superconducting tunnel junction mixer with a normal metal tuning circuit," *Appl. Phys. Lett.*, vol. 68, pp. 1714-1716, March 1996.

[5] W. F. M. Ganzevles, J. R. Gao, D. Wilms Floet, G. de Lange, A. K. van Langen, L. R. Swart, T. M. Klapwijk and P. A. J. de Korte, "Twin-slot antenna coupled Nb hot-electron bolometer mixers at 1 THz and 2.5 THz," *Proceedings of the 10th International Symposium on Space Terahertz Technology,* Charlottesville, VA, March 16-18, pp. 247-260, 1999.

[6] M. Kominami, D. M. Pozar and D. H. Schaubert, "Dipole and slot elements and arrays on semi-infinite substrates," *IEEE Trans. Ant. Propagat.*, vol. 33, pp. 600-607, June 1985. We used a computer code of this method by J. Zmuidzinas and G. Chattopadhyay, California Institute of Technology, Downs Laboratory of Physics, Pasadena, CA 91125.

[7] W. F. M. Ganzevles, J. R. Gao, N. D. Whyborn, P. A. J. de Korte and T. M. Klapwijk, "Novel design for a 2.5 THz quasi-optical hot-electron bolometer mixer," *Proceedings of the ESA Workshop on Millimetre Wave Technology and Applications,* Espoo, Finland, pp. 504-509, June 21-23, 1998.

[8] W. F. M. Ganzevles J. R. Gao, W. M. Laauwen, G. de Lange, T. M. Klapwijk and P. A. J. de Korte, "Direct and heterodyne response of quasi-optical Nb hot-electron bolometer mixers designed for 2.5 Thz radiation detection," *Proceedings of the 11th International Symposium on Space Terahertz Technology,* Ann Arbor, MI, May 1-3, 2000, submitted for publication.

[9] D. M. Pozar, *Microwave Engineering,* Boston: Addison-Wesley, 1990.

[10] G. Yassin and S. Withington, "Electromagnetic models for superconducting millimetre-wave and submillimeter wave microstrip transmission lines", *ESA Technical Report RDG 4*, 1995 and G. Yassin and S. Withington, "Electromagnetic models for superconducting millimetre-wave and sub-millimetre-wave microstrip transmission lines", *J. of Phys. D*, vol. 28, pp. 1983-1991, September 1995.

[11] R. A. Wyss, B. S. Karasik, W. R. McGrath, B. Bumble and H. G. LeDuc, "Noise and bandwidth measurements of diffusion cooled Nb hot-electron bolometer mixers at frequencies above the superconductive energy gap," *Proceedings of the 10th International Symposium on Space Terahertz Technology,* Charlottesville, VA, March 16-18, pp. 215-228, 1999.

[12] R. A. Wyss, A. Neto, W. R. McGrath, B. Bumble and H. G. LeDuc, "Submillimeter-wave spectral response of twin-slot antennas coupled to hot-electron bolometers," *Proceedings of the 11th International Symposium on Space Terahertz Technology,* Ann Arbor, MI, May 1-3, 2000, submitted for publication.